

TiO₂(SiO₂)_x and ZrO₂(SiO₂)_x Cryogels as Catalysts for the Citronellal Cyclization to Isopulegol

Ciril Jimeno · Jonathan Miras · Jordi Esquena

Received: 15 February 2013 / Accepted: 6 April 2013 / Published online: 17 April 2013
© Springer Science+Business Media New York 2013

Abstract TiO₂(SiO₂)_x and ZrO₂(SiO₂)_x mixed oxides prepared by a simple sol–gel procedure plus freeze-drying achieve very high surface areas. Such cryogels are shown to catalyze the cyclization of citronellal to isopulegol. The dispersion of the active metal has been optimized, as it is shown that high specific surface areas are the key for the catalytic activity of the cogels. Nevertheless zirconia–silica cryogels depict much higher catalytic activity, with only 5 mol% Zr being required, than the corresponding titania–silica mixed oxides.

Keywords Titania–silica · Zirconia–silica · Mixed oxides · Isopulegol · Heterogeneous catalysis · Citronellal

1 Introduction

Since the initial discovery by Nakatani and Kawashima [1] that stoichiometric amounts of ZnBr₂ promoted the cyclization of citronellal (Scheme 1) with high diastereoselectivity (ds) towards isopulegol (up to 94 % ds), in what is a key step in the industrial synthesis of (–)-menthol, the

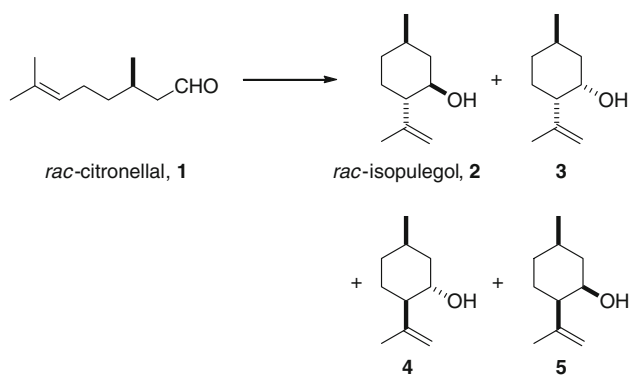
interest in developing heterogeneous catalysts for such transformation has grown because not only typical factors like conversion and chemoselectivity must be controlled, but also the stereoselectivity of the reaction towards the desired diastereomer [2].

The use of porous titania–silica and zirconia–silica mixed oxides prepared through sol–gel procedures in this reaction is attractive because their properties can be easily controlled by fine-tuning their composition and synthesis conditions. In particular, cryogels (like aerogels) offer the possibility of achieving very high specific surfaces since pore collapse is avoided during the drying step [3, 4]. Surprisingly, to our knowledge there is only one preliminary report on the citronellal cyclization that makes use of regular xerogels as catalysts for the cyclization of citronellal: Ravasio et al. [5] showed that commercial TiO₂– and ZrO₂–SiO₂ cogels (100 wt%) were able to perform the reaction at 90 °C, both with moderate diastereoselectivity (62 % ds), but no detailed study was conducted. Other types of zirconium-containing heterogeneous catalysts have received more attention. Zr-exchanged montmorillonite (5 mol% acid sites, 40 wt%) was successfully tested, although only the two main diastereomers were controlled during the research [6]. Sulphated zirconia (10 wt%) gave a poor diastereoselectivity [7, 8]. Hydrous zirconia (5 wt%) was more effective, reaching 72 % ds, which suggests that Lewis acidity, not Brønsted acidity, was crucial for the stereoselectivity [9]. Later Chuah et al. [10] also developed a series of Zr zeolites (8 wt%) able to promote the cyclization with high efficiency (up to 92 % ds), including a subsequent hydrogenation to yield menthol directly [11, 12]. Finally, the mesoporous silica Zr-TUD-1 (16 wt%) has also been shown to catalyze this reaction, with 69 % diastereoselectivity [13–15]. In all cases, relatively high temperatures ranging from 80 to 110 °C were used. Herein

Electronic supplementary material The online version of this article (doi:10.1007/s10562-013-1007-5) contains supplementary material, which is available to authorized users.

C. Jimeno (✉)
Department of Biological Chemistry and Molecular Modelling,
Institute of Advanced Chemistry of Catalonia (IQAC-CSIC),
c/Jordi Girona 18-26, 08034 Barcelona, Spain
e-mail: ciril.jimeno@iqac.csic.es

J. Miras · J. Esquena
Department of Chemical and Biomolecular Nanotechnology,
Institute of Advanced Chemistry of Catalonia (IQAC-CSIC),
c/Jordi Girona 18-26, 08034 Barcelona, Spain



Scheme 1 Cyclization of citronellal to isopulegol plus diastereomers

we want to present our study of zirconia–silica and titania–silica cryogels with high specific surface areas for this reaction.

2 Experimental

2.1 Materials and Methods

Tetraethoxysilane (TEOS) and titanium(IV) tetraisopropoxide were purchased from Aldrich, and used as received. Zirconium(IV) tetra(n-butoxide) was purchased from Strem. Absolute ethanol (analysis grade, from Merck Chemicals), concentrated hydrochloric acid (37 %, analysis grade, from Acros) and MilliQ water (18.2 MΩ cm) were used for the preparation of mixed oxides. Anhydrous dichloromethane obtained from a solvent purification system was used for the carbonyl-ene reactions.

X-ray analyses were carried out at Servei de Difracció de Raigs-X from Institut de Ciències de la Terra Jaume Almera (ICTJA-CSIC, Barcelona) by combination of X-ray powder diffraction (XRD) and X-ray fluorescence (XRF) measurements. XRD scans were acquired with a Bruker-AXS (Siemens) D5005 powder diffractometer equipped with a 2.2 kW sealed Cu X-ray source, a graphite monochromator and a NaI(Tl) scintillation detector. To determine the amorphous content of the samples with the Rietveld method, the samples were spiked with a known proportion of internal standard (20 % of CaF₂ in weight). XRF measurements were carried out with a Panalytical Axios PW 4400/40 sequential wavelength dispersive spectrometer. Transmission electron microscope (TEM) images were recorded at Serveis Científic-Tècnics of the Universitat de Barcelona. Samples were analysed in a carbon holder by using a Hitachi (model H-800-MT) TEM operated at 200 kV. For the energy-dispersive X-ray microanalysis (EDX) an X-ray Silicon Drift Chamber detector (Bruker, 133 eV resol.) was used. The STEM mode used a spot size 10–15 nm and a beam current of 15 μA. Nitrogen sorption experiments were performed in

a Quantachrome Autosorb-IQ automated gas sorption apparatus. Samples were degassed at 80 °C for 24 h before the experiments, and N₂ sorption isotherms were recorded at –196 °C. NMR analyses were performed in an automated Varian VNMRS 400 MHz equipped with an One NMR Probe. CDCl₃ was used as solvent and reference. FTIR spectra (KBr pellets) were recorded in a Nicolet Avatar 360 apparatus.

2.2 Preparation of the Catalysts, Ti–Six and Zr–Six

TiO₂(SiO₂)_x and ZrO₂(SiO₂)_x cogels of variable composition (molar ratio of the precursors $x = 1, 2, 4, 8,$ and 16) were synthesized as described elsewhere [16]. The cogels obtained were frozen, and then lyophilized. The final cryogels were ground to a fine powder and heated at 80 °C under high vacuum (<1 mbar) for 24 h. Hereafter, these materials will be named Ti–Six and Zr–Six, where x can range from 1 to 16 and refers exclusively to the molar ratio of the precursors.

2.3 Citronellal Cyclization, Typical Procedure

33 mg of Zr–Si8 catalyst (5 mol% Zr with respect to citronellal) was weighed into a flame-dried flask, and purged with nitrogen. 4 mL anhydrous dichloromethane was added via syringe. Then, citronellal (200 μL, 1.10 mmol) was added, and the mixture was stirred at room temperature (rt) for 20 h. The suspension was filtered through a pad of Celite 545 and washed thoroughly with CH₂Cl₂. After solvent removal in vacuo, the crude product was analyzed by ¹H-NMR to determine conversion and diastereoselectivity by integration of characteristic signals [17]. Purification, when required, was carried out by flash chromatography on silica gel, eluting with hexane.

3 Results and Discussion

3.1 Characterization of Materials

The as synthesized materials were first analyzed by X-ray diffraction, which indicated that anatase was the only crystalline phase present in the Ti–Six mixed oxides, whereas Zr–Six materials were amorphous (See supplementary material). Quantitative Rietveld analysis combined with X-rays fluorescence established the amounts of anatase, total titania, zirconia, and silica. A sample of pure silica was also prepared and characterized using the same procedure, for comparison purposes. These data are summarized in Table 1. Incorporation of both titania and zirconia into the silica matrix was very efficient, yielding materials with MO₂/silica ratios certainly close to the

Table 1 X-rays characterization of $\text{TiO}_2(\text{SiO}_2)_x$ and $\text{ZrO}_2(\text{SiO}_2)_x$ mixed oxides

Catalyst	Anatase (wt%) ^a	Total titania or zirconia (wt%) ^b	Anatase/total titania%	Nominal MO_2/SiO_2 wt ratio	Determined MO_2/SiO_2 wt ratio ^b
Silica	0	0	na	na	na
Ti–Si1	23.7	47.1	50.3	1.33	1.32
Ti–Si2	16.7	33.3	50.1	0.67	0.66
Ti–Si4	7.9	21.7	36.4	0.33	0.35
Ti–Si8	3.9	12.0	32.5	0.17	0.17
Zr–Si2	na	45.8	na	1.03	1.10
Zr–Si4	na	33.9	na	0.51	0.58
Zr–Si8	na	20.4	na	0.26	0.30
Zr–Si16	na	11.4	na	0.13	0.15

^a Determined by X-ray Rietveld analysis

^b Determined by X-ray fluorescence analysis

nominal values. However, when the crystalline titania percentage was calculated over the total titania amount, it was evident that different results were obtained depending on the stoichiometry of the mixed oxide. Thus, Ti–Si1 and Ti–Si2 gave an even distribution of crystalline (anatase) versus amorphous titania (ca. 50 wt% anatase over total titania), whereas materials with lower Ti/Si ratios, Ti–Si4 and Ti–Si8, yielded crystalline/amorphous titania ratios of ca. 1/2 (only ca. 33 wt% anatase over total titania, Table 1). An increase in the amount of silica matrix results into the suppression of crystallization of the minor component (TiO_2). Therefore, a significant increase in the amorphous titania fraction was achieved upon dilution in the silica matrix during the synthesis.

Then, textural studies concluded that such cryogels contained both micropores and mesopores. Table 2 shows that the specific surface area (SSA) determined by the BET method was large ($>1,000 \text{ m}^2/\text{g}$) for Ti–Si2, Ti–Si4, and Ti–Si8, whereas a lower value was obtained for the 1:1 $\text{TiO}_2:\text{SiO}_2$ material ($744 \text{ m}^2/\text{g}$). Total pore volumes ranged between $0.6\text{--}0.9 \text{ cm}^3/\text{g}$. Pore widths were then obtained by the Density Functional Theory (DFT) method [18]. For the 1:1 $\text{TiO}_2:\text{SiO}_2$ composite, they were similar to pure silica, but the pore width was much smaller for the other compounds, around 1.3 nm. Finally, surface due to microporosity, determined by the t-plot method [19], increased steadily up to a maximum for Ti–Si8 ($690 \text{ m}^2/\text{g}$).

Similarly, although SSA areas are lower for the Zr–Six cryogels due to the higher atomic weight of zirconium, they increased upon dispersion of zirconia, from $380 \text{ m}^2/\text{g}$ in Zr–Si2 to $914 \text{ m}^2/\text{g}$ for Zr–Si16. Total pore volumes ranged from 0.4 to $0.8 \text{ cm}^3/\text{g}$, whereas pore diameters decreased from 3.5 nm in Zr–Si4 down to 1.4 nm in Zr–Si16. As for Ti–Si_x materials, microporosity surface

Table 2 Textural characterization of $\text{TiO}_2(\text{SiO}_2)_x$ and $\text{ZrO}_2(\text{SiO}_2)_x$ mixed oxides

Catalyst (MO_2 wt%)	S_{BET}^a (m^2/g)	V_{p}^b (cm^3/g)	D_{p}^c (nm)	S_{Micro}^d (m^2/g)
Silica	1,316	1.17	3.2	236
Ti–Si1 (47 %)	744	0.76	3.8	136
Ti–Si2 (33 %)	1,032	0.89	1.3	463
Ti–Si4 (22 %)	1,093	0.79	1.3	556
Ti–Si8 (12 %)	1,032	0.62	1.4	690
Zr–Si2 (46 %)	380	0.36	2.6	81
Zr–Si4 (34 %)	667	0.76	3.5	86
Zr–Si8 (20 %)	696	0.56	2.6	131
Zr–Si16 (11 %)	914	0.84	1.4	427

^a SSA determined by the BET isotherm method

^b Total pore volume

^c Pore width according to the DFT method applied to the adsorption branch

^d Estimated micropore area determined by the t-plot method

always increased upon dispersion of zirconia in silica, reaching $427 \text{ m}^2/\text{g}$ for Zr–Si16. Altogether these data indicated that dispersion of titania and zirconia into the silica matrix produced an increase in the surface area, especially compared to the more concentrated materials Ti–Si1 and Zr–Si2, which contain about 50 wt% of titania or zirconia, respectively, due to a smaller D_{p} , and the general increase of microporosity.

Afterwards, TEM images were taken in search of the nanocrystalline part of the Ti–Six composites. Small nanoparticles in the range $5\text{--}10 \text{ nm}$ could be clearly seen. In general, these nanoparticles corresponding to anatase showed good dispersion in the silica matrix but some tendency to self-aggregation: sometimes two or more anatase nanoparticles appeared attached. In Fig. 1, some representative TEM images are shown.

Since Zr–Six materials were completely amorphous, an elements mapping (EDX experiment) was carried out in STEM mode to assess whether well mixed zirconia or segregated domains were present. Images shown in Fig. 2 indicate that a good dispersion of zirconia was achieved indeed, as Zr, Si and O appear homogeneously distributed at the scale analyzed.

3.2 Catalytic Experiments

Since all cryogels had been synthesized at $80 \text{ }^\circ\text{C}$ maximum (gelation temperature), we decided to carry out the catalytic tests at room temperature to avoid any potential degradation of the catalyst during the reactions. Ti–Six catalysts were first tested in the cyclization of citronellal. We were pleased to find that the cyclization to isopulegol took place in CH_2Cl_2 smoothly. However, high catalyst

Fig. 1 Representative TEM images of Ti–Si4 (a), and Ti–Si8 (b). Arrows highlight some of the nanocrystallites

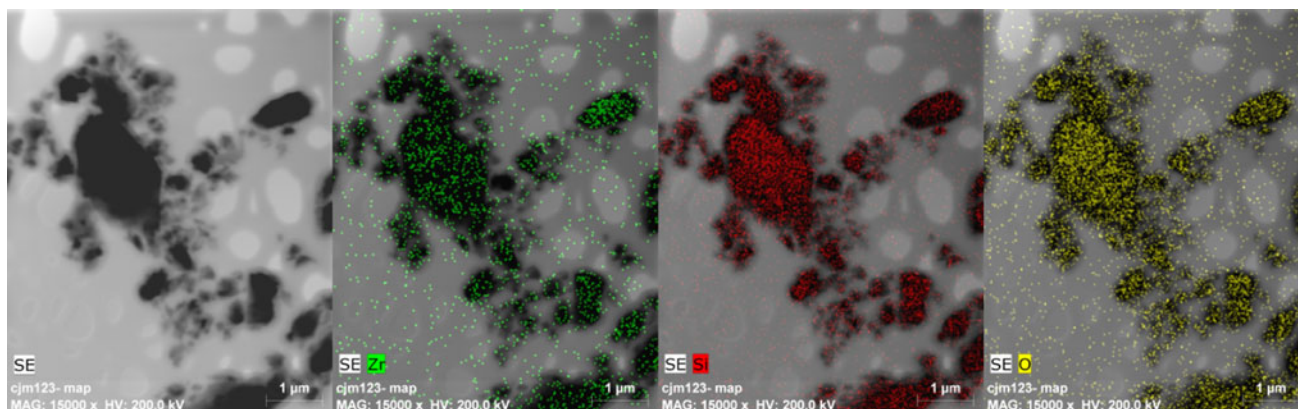
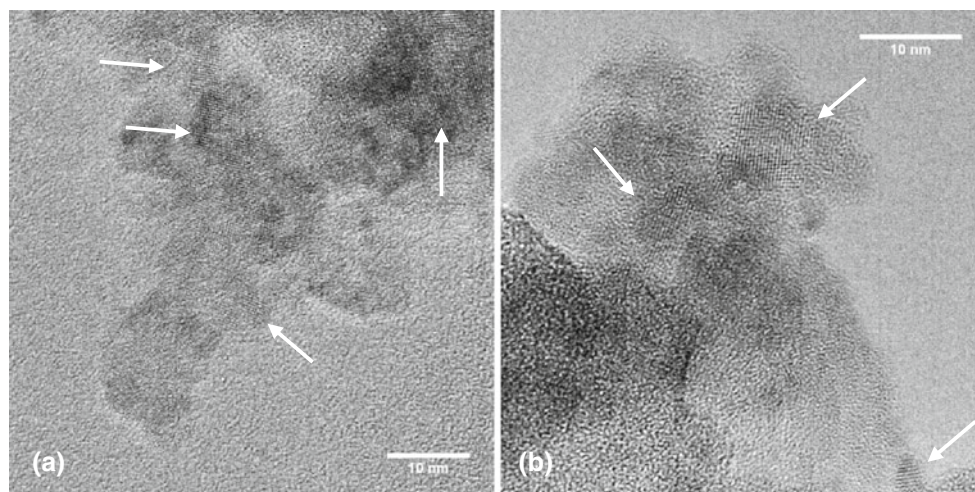


Fig. 2 TEM and Zr, Si, and O EDX images of Zr–Si8 at magnification $\times 15,000$

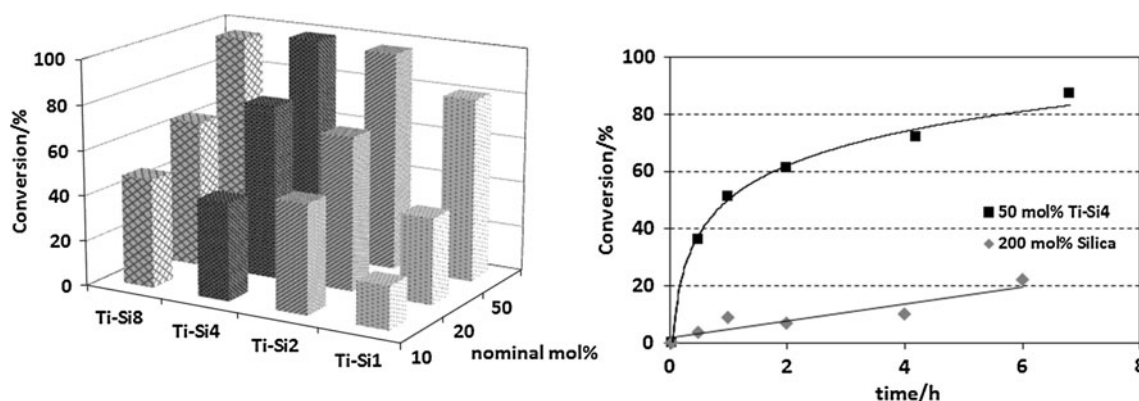


Fig. 3 Citronellal conversion for catalysts Ti–Si_x after 20 h at rt in dichloromethane, with increasing nominal catalyst loadings with respect to citronellal (left). Conversion versus time for equivalent

amounts of Ti–Si₄ and Silica, at room temperature (right). Conversion determined by ¹H-NMR

loadings were needed. At catalyst loadings of 10 mol% Ti with respect to citronellal, incomplete conversions were achieved, and finally, 50 mol% of Ti loadings were used.

Furthermore, catalysts with higher titania dispersion were more effective than the 1:1 cryogel. Maximum conversion in the benchmark reaction was indeed achieved for

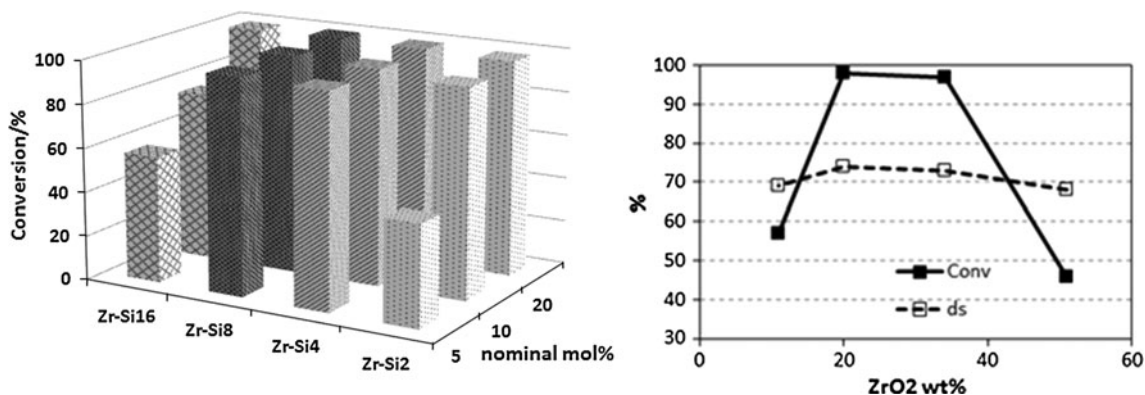


Fig. 4 Citronellal conversion for catalysts Zr-Six after 20 h at rt in dichloromethane, with increasing nominal catalyst loadings (left). Dependency of citronellal conversion and diastereoselectivity (ds)

with ZrO₂ wt% in catalysts Zr-Six after 20 h at rt in dichloromethane, with 5 mol% Zr loadings (right). Conversion and ds determined by ¹H-NMR

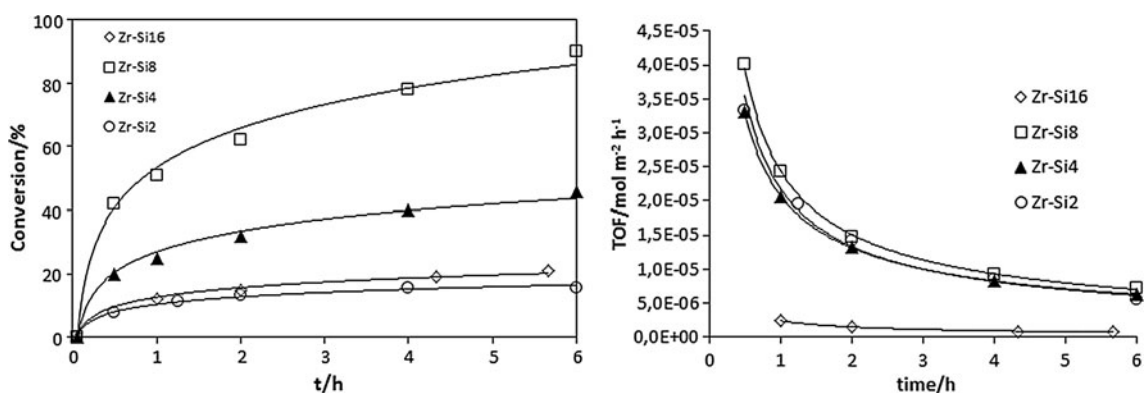


Fig. 5 Conversion versus time plot for Zr-Six mixed oxides (left), and TOF versus time plot for Zr-Six mixed oxides (right), at rt and 5 mol% Zr loading

50 mol% of Ti-Si4 (99 % conversion) whereas Ti-Si2 and Ti-Si8 activities remained slightly below (Fig. 3, left). No other by-products were observed.

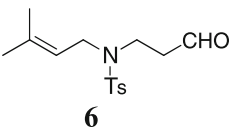
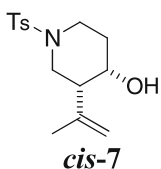
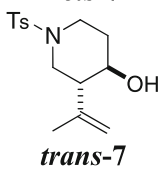
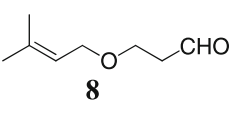
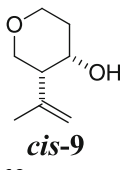
When the diastereoselectivity (ds) towards isopulegol was analyzed, it was found that differences between the nano-composites were small, in the range of 5 %. Catalysts Ti-Si1 and Ti-Si8 showed the poorest behaviour, and diastereoselectivity was just 59 %. Mixed oxides with 1:2 and 1:4 TiO₂:SiO₂ ratios showed the most stable and highest stereoselectivity, near 65 % ds, for the whole range of catalyst loadings studied. Taking into account both conversion and diastereoselectivity, titania dispersed in silica in a 1:4 ratio (Ti-Si4) is the most reliable combination at 50 mol% loading, yielding isopulegol in 99 % conversion and 64 % ds at room temperature, followed by Ti-Si2 (97 % conversion, 63 % ds). It is also worth mentioning that at 60 °C (not shown in Fig. 3), 20 mol% of Ti-Si4 was able to promote the conversion of citronellal in 93 % conversion after 7 h (reaction carried out in a sealed tube) while still keeping 62 % ds.

The possibility of a significant background reaction due to silica catalysis was then studied [17]. Conversion and

selectivity values from Ti-Si4 were compared to data collected from a four-fold molar amount of silica prepared by the same method (Fig. 3, right). A conversion versus time plot using 50 mol% of Ti-Si4 and 200 mol% Silica demonstrated that the TiO₂-SiO₂ cogel was an active promoter of the reaction, reaching more than 80 % conversion after 7 h, whereas the equivalent amount of pure silica barely achieved 20 % conversion in 6 h. Moreover, diastereoselectivity using Silica never surpassed 50 %, compared to 64 % with Ti-Si4.

Next, Zr-Six cogels were tested (Fig. 4, left). Much higher levels of catalytic activity were observed than for Ti-Six under identical reaction conditions. All materials gave conversions >98 % at 20 mol% Zr loading. At lower loadings differences in performance arose again, and at 5 mol% zirconium loading, Zr-Si4 and Zr-Si8 stood up, still achieving 97 and 98 % conversion respectively. Even more interestingly, diastereoselectivity towards isopulegol was also higher for these series of catalysts than for Ti-Six, 68 % ds for Zr-Si2, 73 % ds for Zr-Si4, 74 % ds for Zr-Si8, and 69 % ds for Zr-Si16. These results clearly show

Table 3 Molecular probes for Ti–Si4 and Zr–Si8 acidity

Probe	Catalyst (M mol% loading)	Predominant product ^a	Conv.(%) ^a	<i>cis/trans</i> dr ^a
 6	Ti–Si4 (50 %)	 <i>cis</i>-7	50 ^b 98 ^c (79) ^e	1.4/1
	Zr–Si8 (5 %)	 <i>trans</i>-7	83 ^b	1/1.1
 8	Ti–Si4 (20 %)	 <i>cis</i>-9	71 ^d	1.2/1
	Zr–Si8 (10 %)	None	83 ^b	1.0/1

^a Determined by ¹H-NMR^b At rt for 20 h^c At 60 °C for 16 h^d At 60 °C for 7 h^e Isolated yield

the influence of the dispersion of zirconia into the silica up to an optimal point, reached around 20 wt% (Zr–Si8), as illustrated in Fig. 4, right. Again, total selectivity towards cyclization products was observed.

An initial kinetic analysis of the different Zr-containing catalysts suggested that differences between them were actually bigger than shown through conversion and *ds* values: indeed, Zr–Si8 was quite faster than Zr–Si4, and left far behind Zr–Si2 and Zr–Si16, showing the importance of metal dispersion on silica to control catalysis (Fig. 5, left). Zr–Si8 yielded more than 80 % isopulegol in 6 h at room temperature, at just 5 mol% Zr loading. In order to obtain a more accurate analysis, turnover frequencies (TOF) were calculated as moles of citronellal converted per gram of catalyst used per specific surface area (SSA) per hour, and plotted as a function of time (Fig. 5, right). The plots for the different mixed oxides overlaid very nicely except for Zr–Si16, thus disclosing that, with a minimum concentration of available Zr active sites, catalytic performance depended basically on the SSA available of the catalyst. Hence, Zr–Si2, Zr–Si4 and Zr–Si8 were shown to have indeed identical catalytic activity. The observed rate increase upon dispersion on silica (Zr–Si8 > Zr–Si4 > Zr–Si2) arose simply from the increase in SSA. This trend breaks for Zr–Si16 (11 wt% ZrO₂), where

further dispersion seemed to inhibit catalysis, likely due to a diminished pore diameter (*D_p* = 1.4 nm, Table 2) and the burial of Zr sites into the silica matrix at higher Si/Zr ratios. Therefore the optimal catalytic performance must come from a compromise between the highest SSA possible for the catalyst (mainly due to the increase of microporosity with increasing ZrO₂- or TiO₂-dispersion) and the decrease of active sites concentration due to dispersion itself.

Finally, recycling experiments were carried out with the Zr–Si8 cryogel: after the reaction, the reaction medium was diluted with CH₂Cl₂, centrifuged at 4,000 rpm, and decanted. The remaining solid was washed-centrifuged-decanted again and finally dried at 80 °C, and reused. In this way, only a slight decrease in activity was observed after 3 cycles, still yielding 92 % conversion, whereas diastereoselectivity remained constant.

3.3 Origin of Diastereoselectivity With Molecular Probes

It is well known that titania- and zirconia-silica cogels present Brønsted acidity due to the presence of silanol and M–OH groups as well as Lewis acidity because of the M⁴⁺ centers [20–29]. Indeed, pyridine adsorption/desorption

FTIR spectra and TGA of selected samples with and without adsorbed pyridine show that a variety of acidic sites (Lewis and Brønsted) are present in the catalysts (See Electronic Supplementary Material). We have also established in this work that silica itself is barely able to promote the carbonyl-ene cyclization of citronellal, even at high loadings (200 mol%) (Fig. 4), and therefore the activity of silanol groups is negligible. It is reasonable to attribute the higher diastereoselectivity of Zr–Six cryogels (compared to Ti–Six) to an enhanced Lewis acidity [2], either due to a higher amount of Lewis acid sites or to their improved accessibility to citronellal. To probe this idea, we decided to use the carbonyl-ene reaction itself: it had been established that certain enals yield specifically *cis* cyclization products from the action of Brønsted acids whereas Lewis acids promote *trans* cyclizations [30, 31]. Accordingly, we decided to use enals **6** and **8** as molecular probes to evaluate the origin of the observed diastereoselectivity (Table 3).

Thus we observed that using Ti–Si₄, the *N*-tosyl derivative **6**, yielded the *cis* isomer with a small predominance. The ether version, **8** [32], confirmed the observation and also afforded the cyclization product in good yield with slight *cis* predominance. On the other hand, Zr–Si₈ yielded cyclization products from **6** with some *trans* predominance, and unlike for Ti–Si₄, **8** was converted to an even mixture of *cis* and *trans* products. It is thus suggested that although both Brønsted and Lewis acidity coming from the active metal are operative in these carbonyl-ene reactions, Zr–Six cryogels exhibit a slight predominance of Lewis acidity with respect to Ti–Six, which leads to a higher proportion of *trans* products, and therefore to a higher ratio of isopulegol with respect to the other isomers (from 62 % ds for Ti–Si₄ to 74 % ds for Zr–Si₈) [2].

4 Conclusion

Titania- and zirconia-silica cryogels of different ratios have been prepared and successfully tested as catalysts in carbonyl-ene cyclizations at room temperature. Although the performance of Ti–Six is modest, zirconia-silica cogels show excellent catalytic activity, and diastereoselectivities up to 74 % ds, with a loading of just 5 mol% Zr. The Zr–Si₈ mixed oxide was found optimal for this reaction. Moreover, we have established that the performance of such catalysts is due to their high specific surface areas, which can be controlled and therefore optimized by tuning the ratio of zirconia into the silica matrix during their synthesis.

The background reaction due to silica catalysis was found to be slow, affecting slightly the performance of Ti–

Six catalysts, but it can be considered negligible for the faster Zr–Six materials. The use of molecular probes suggested that the observed diastereoselectivity was due to a combination of Brønsted and Lewis acidity, even though Lewis acidity predominated slightly in Zr–Six cryogels. This accounts for the enhanced diastereoselectivity of such Zr cryogels.

Acknowledgments Financial support comes from Ministerio de Economía y Competitividad (CTQ2012-38594-C02-02 and RYC-2010-06750). CJ is a Ramón y Cajal fellow. Support by Prof. A. Messeguer and Prof. I. Alfonso is deeply acknowledged.

References

- Nakatani Y, Kawashima K (1978) *Synthesis*:147
- Boronat M, Corma A, Renz M (2008) In: Harris KDM, Edwards PP (eds) *Turning points in solid-state, materials and surface science*. RSC Publishing, Cambridge, p 639
- Pajonk GM (1997) *Catal Today* 35:319
- Pons A, Casas L, Estop E, Molins E, Harris KDM, Xu M (2012) *J Non-Cryst Solids* 358:461
- Ravasio N, Antenori M, Babudri F, Gargano M (1997) *Stud Surf Sci Catal* 108:625
- Tateiwa J, Kimura A, Takasuka M, Uemura S (1997) *J Chem Soc Perkin Trans 1*:2169
- Yadav GD, Nair JJ (1998) *Chem Commun*:2369
- Yadav GD, Nair JJ (2000) *Langmuir* 16:4072
- Chuah GK, Liu SH, Jaenicke S, Harrison LJ (2001) *J Catal* 200:352
- Zhu YZ, Nie YT, Jaenicke S, Chuah GK (2005) *J Catal* 229:404
- Nie Y, Niah W, Jaenicke S, Chuah G-K (2007) *J Catal* 248:1
- Nie Y, Jaenicke S, Chuah G-K (2009) *Chem Eur J* 15:1991
- Telalovic S, Ng JF, Maheswari R, Ramanathan A, Chuah GK, Hanefeld U (2008) *Chem Commun*:4631
- Ramanathan A, Villalobos MCC, Kwakernaak C, Telalovic S, Hanefeld U (2008) *Chem Eur J* 14:961
- Telalovic S, Ramanathan A, Ng JF, Maheswari R, Kwakernaak C, Soulimani F, Brouwer HC, Chuah GK, Weckhuysen BM, Hanefeld U (2011) *Chem Eur J* 17:2077
- Cernuto G, Galli S, Trudu F, Colonna GM, Masciocchi N, Cervellino A, Guagliardi A (2011) *Angew Chem Int Ed* 50:10828
- Kropp PJ, Breton GW, Craig SL, Crawford SD, Durland WF, Jones JE, Raleigh JS (1995) *J Org Chem* 60:4146
- Ravikovitch PI, Odomehnaill SC, Neimark AV, Schuth F, Unger KK (1995) *Langmuir* 11:4765
- de Boer JH, Lippens BC, Linsen BG, Broekhof JCP, Van den Heuvel A, Osinga TJ (1966) *J Colloid Interface Sci* 21:405
- Liu J, Kosuda KM, Van Duyne RP, Stair PC (2009) *J Phys Chem C* 113:12412
- Ren J, Li Z, Liu S, Xing Y, Xie K (2008) *Catal Lett* 124:185
- Bonelli B, Cozzolino M, Tesser R, Di Serio M, Piemetti M, Garrone E, Santacesaria E (2007) *J Catal* 246:293
- Sidhpuria KB, Tyagi B, Jasra RV (2011) *Catal Lett* 141:1164
- Tyagi B, Sidhpuria KB, Shaik B, Jasra RV (2010) *J Porous Mater* 17:699
- Rodriguez Avendano RG, De Los Reyes JA, Viveros T, Montoya De La Fuente JA (2009) *Catal Today* 148:12
- Viter VN (2010) *Russ J Appl Chem* 83:195
- Viter VN (2009) *Pol J Chem* 83:1515

28. Avendano RGR, de los Reyes JA, Montoya JA, Viveros T (2005) *J Sol-Gel Sci Technol* 33:133
29. Soled S, McVicker GB (1992) *Catal Today* 14:189
30. Williams JT, Bahia PS, Snaith JS (2002) *Org Lett* 4:3727
31. Williams JT, Bahi PS, Kariuki BM, Spencer N, Philp D, Snaith JS (2006) *J Org Chem* 71:2460
32. Grise CM, Rodrigue EM, Barriault L (2008) *Tetrahedron* 64:797